J. Mol. Biol. (1997) **272**, 633–641

JMB

Helix-helix Packing in a Membrane-like Environment

Ismael Mingarro, Arne Elofsson and Gunnar von Heijne*

Department of Biochemistry Stockholm University, S-106 91 Stockholm, Sweden

The unique ability of the glycophorin A transmembrane helix to dimerize in SDS has previously been exploited in studies of the sequence specificity of helix-helix packing in a micellar environment. Here, we have made different insertion mutants in the critical helix-helix interface segment, and find that efficient dimerization can be mediated by a wider range of sequence motifs than suggested by the earlier studies. We also show that certain mutants that are unable to dimerize can nevertheless form relatively high amounts of tetramers, and that specific tetramerization can be induced by duplication of the critical interface motif on the lipid-exposed side of the transmembrane helix.

© 1997 Academic Press Limited

*Corresponding author

Keywords: membrane protein; helix packing; glycophorin A

Introduction

Due in part to the difficulty of obtaining high-resolution structures of integral membrane proteins, the seemingly simple problem of understanding the structural and energetic basis for specific packing between transmembrane helices in a lipid environment is largely unresolved (Lemmon & Engelman, 1994). One of the few available systems that allow questions of this kind to be addressed in a relatively straightforward way is that based on the SDS-resistant dimerization of the glycophorin A (GpA) transmembrane helix (Lemmon *et al.*, 1992a). Exhaustive random mutagenesis studies have made it possible to construct a detailed model of the GpA dimer where seven residues on one face of the transmembrane helix mediate the helix-helix interaction (Adams *et al.*, 1996; Langosch *et al.*, 1996; Lemmon *et al.*, 1992b, 1994; Treutlein *et al.*, 1992; Figure 1); this model has recently been confirmed by NMR structure determination (MacKenzie *et al.*, 1997).

We have previously shown that the critical packing region in the GpA transmembrane helix can be identified not only by replacement mutagenesis but also, and more rapidly, by an insertion mutagenesis approach (Mingarro *et al.*, 1996). The insertion of a single alanine into a number of positions in the segment of the helix containing the seven critical residues predictably resulted in disruption of the dimer, whereas insertions outside this segment had little or no effect.

In an effort to further characterize the GpA dimer interface, we now report on the effects of insertion mutants where up to ten contiguous alanine, glycine or leucine residues have been inserted into the middle of the critical segment. Although many of these constructs do not dimerize in SDS, a surprisingly large number form dimers with almost the same efficiency as the wild-type protein, suggesting that the sequence requirements for dimer formation may not be as stringent as initially thought.

Unexpectedly, certain mutants were found to form SDS-resistant tetramers with rather high efficiency. Two of these mutants could only form monomers and tetramers (but not dimers), suggesting co-operativity in the formation of the helix bundle. Tetramer formation could also be induced by duplicating the dimer interface motif on the opposite side of the GpA transmembrane helix. These results suggest that efficient structural engineering of integral membrane proteins may be within reach.

Abbreviations used: GpA, glycophorin A.

Results

Multiple Ala and Leu-insertions reveal new possibilities for helix-helix packing

For these studies, the experimental approach was the same as used previously, i.e. a C-terminal fragment of GpA (residues 60 to 131) including the transmembrane segment or mutants thereof were expressed in *Escherichia coli* as C-terminal fusions to staphylococcal nuclease, and were purified in one step using Ni^{+}-chelating affinity purification and a C-terminal His_6-tag (Mingarro *et al.*, 1996). The purified proteins were adjusted to a 25 μM concentration in 2% (w/v) SDS and were analyzed by SDS-PAGE. As shown in Figure 2 (lane 2), the

0022–2836/97/390633–09 $25.00/0/mb971276

© 1997 Academic Press Limited

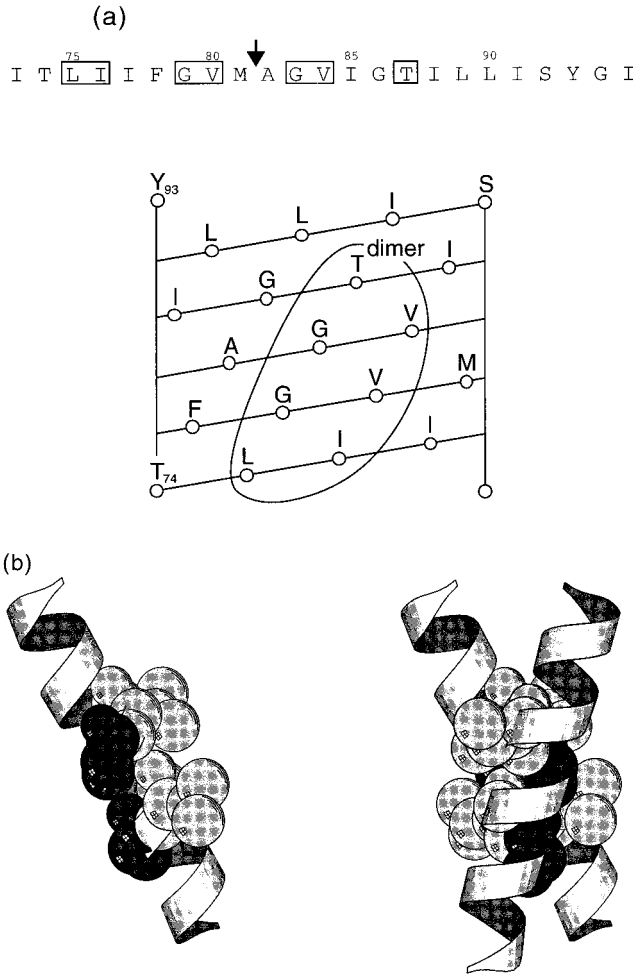

Figure 1. (a) Sequence of the wild-type GpA transmembrane helix. At the top the seven critical interface residues defined by replacement mutagenesis (Lemmon *et al.*, 1992b) and NMR spectroscopy (MacKenzie *et al.*, 1997) are boxed. The arrow marks the point where amino acid insertions were made in this study. The bottom shows the helical net plot where the interface residues are outlined. (b) Model of the GpA momomer (left) and dimer (right) (Adams *et al.*, 1996). The orientation is the same in both models, i.e. one is looking into the interface in the monomer model. Glycine residues 79 and 83 in each helix are shown in space-filling mode in dark grey, and valine 80 and 84 in light grey. The N termini are at the bottom. 3D-models were visualized using MOLSCRIPT (Kraulis, 1991).

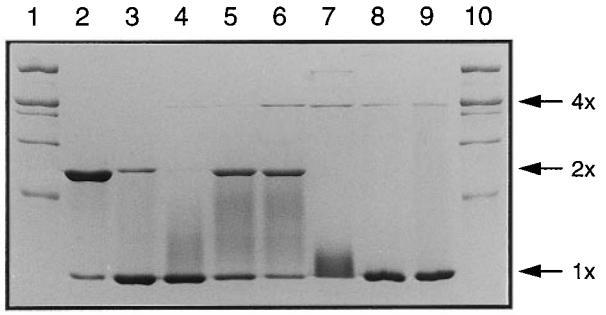

Figure 2. SDS-PAGE analysis of Ala-insertion mutants, the insertion point is shown in Figure 1(a). Lanes 1 and 10 show high molecular mass markers (Bio-Rad) of 200, 116, 97.4, 66 and 45 kDa. Lane 2: nuclease-GpA wild-type fusion protein. Lanes 3 to 9: mutants with one to seven inserted alanine residues. Monomers (1×), dimers (2×), and tetramers (4×) are indicated.

wild-type GpA sequence dimerizes very efficiently (83% dimer) under these conditions.

In an attempt to create new dimer interfaces, one to ten alanine residues were inserted into the middle of the segment encompassing the seven critical interface residues (between residues Met81 and Ala82), Figure 1(a). As expected, most of these mutants did not form dimers; however, mutants 3A and 4A both dimerized nearly as efficiently as the wild-type (Figure 2 and Table 1). Notably, mutants 4A and 5A also formed detectable amounts of tetramer.

Since insertion of three or four alanine residues, roughly one helical turn, will tend to restore the relative positioning of the residues on either side of the insertion, it was of interest to determine whether the residues identified as critical for dimerization of the wild-type GpA segment also were involved in the dimerization of the 3A and 4A mutants. To this end, Gly79 and Gly83, the two most tightly packed residues in the wild-type GpA interface (MacKenzie *et al.*, 1997), were replaced by leucine. As in the wild-type, the Gly83 → Leu replacement disrupted both the 3A and 4A dimers (Figure 3). In contrast, neither of the two Gly79 → Leu mutations disrupted dimerization, though some of the dimer shifted to a tetrameric form in the 3A(G79L) construct.

To further map the interface residues, residues Val80 to Ala82 and Val84 (including the four inserted alanine residues) were individually changed to Trp and Thr87 was changed to Leu in the 4A(G79L) construct, since this construct gave the highest amount of dimer (Table 1). Trp-scanning has been promoted on the basis that the introduction of the very bulky Trp residue into a helix-helix interface should be highly disruptive, whereas it should have no effect when introduced in lipid-exposed (or, in our case, detergent-exposed) locations (Sharp *et al.*, 1995a,b). Indeed, although not all residues in the wild-type GpA helix have been replaced by Trp, the available data is in accord with this expectation (Lemmon *et al.*, 1992b). To replace Thr87, we chose Leu rather than Trp since Thr87 → Leu is known to be highly disruptive in wild-type GpA, whereas Trp has not been tested in this position (Lemmon *et al.*, 1992b).

Dimer formation was strongly reduced or totally abolished in mutants 4A(G79L,V80W), 4A(G79L,V84W), and 4A(G79L,T87L) (Table 1). Unexpectedly, efficient tetramer formation was observed in the 4A(G79L,V80W) and 4A(G79L,T87L) mutants (51% and 36% tetramer, respectively); this is discussed further below. We conclude that, as

Table 1. Fraction of dimer and tetramer for GpA mutants

Mutant	Sequence	% Dimer	% Tetramer
	75 79 83 87		
Wild-type	tLIifGVmaGVigTi d n−	83	0
1A	lIIfgVM**a**aGVigTi dn −s	11	0
2A	iIFgvM**Aa**aGVigTi ss ss	0	0
3A	iFGvm**AAa**aGVigTi ns ss	53	0
4A	fGVm**aAAa**aGVigTi nd ss	62	7
5A	gVM**aaAAa**aGVigTi sn ss	0	5
6A	vM**AaaAAa**aGVigTi dn ss	0	2
7A	m**AAaaAAa**aGVigTi dn ss	0	3
8A	**aAAaaAAa**aGVigTi dn ss	0	0
9A	**aAAaaAAa**aGVigTi dn ss	0	0
10A	**aAAaaAAa**aGVigTi sw ss	0	0
3A(G79L)	iF**L**vm**AAa**aGVigTi ss ss n	35	21
3A(G83L)	iFGvm**AAa**a**L**VigTi s ss	3	0
4A(G79L)	f**L**Vm**aAAa**aGVigTi ns ss n	68	10
4A(G83L)	fGVm**aAAa**a**L**VigTi d ss	2	0
4A(G79L,V80W)	f**LW**m**aAAa**aGVigTi s ss	6	51
4A(G79L,M81W)	f**L**V**w**a**AAa**aGVigTi s ss	71	11
4A(G79L,A1W)	f**L**Vm**w**A**Aa**aGVigTi s −s	44	39
4A(G79L,A2W)	f**L**Vm**aWAa**aGVigTi s sn	40	35
4A(G79L,A3W)	f**L**Vm**aAWa**aGVigTi s ss	87	3
4A(G79L,A4W)	f**L**Vm**aAAw**aGVigTi s ss	82	2
4A(G79L,A82W)	f**L**Vm**aAAaw**GVigTi s ss n	45	28
4A(G79L,V84W)	f**L**Vm**aAAa**aG**W**igTi s ss n	0	10
4A(G79L,T87L)	f**L**Vm**aAAa**aGVig**L**i sw ss	9	36
3A(G79L,V80W)	iF**Lw**m**AAa**aGVigTi nd s	44	2
5G	gVM**ggGGg**aGVigTi nd nw	3	0
5L	gVM**llLLl**aGVigTi nd nw	44	4
5L(G79L)	lVM**llLLl**aGVigTi nd nw n	37	5
5L(G83L)	gVM**llLLl**a**L**VigTi nd nw	2	0
5L(A1)	gVM**alLLl**aGVigTi nd nw	45	5
5L(A2)	gVM**laLLl**aGVigTi nd sw	45	8
5L(A3)	gVM**llALl**aGVigTi nd ns	52	10
5L(A4)	gVM**llLAl**aGVigTi nd nw	25	20
5L(A5)	gVM**llLLa**aGVigTi nd sw	41	5
5A(L4)	gVM**aaALa**aGVigTi	53	0

Residues in positions corresponding to the wild-type interface (assuming that the C-terminal G83V84xxT87 motif is critical in all cases; see the text) are shown in upper case, other residues are in lower case. Mutated residues are in bold and inserted residues are underlined. The amount of dimer found for single-site mutants in corresponding positions relative to Gly83 in wild-type GpA is indicated above each mutated residue using a qualitative scale (Lemmon *et al.*, 1992b): n, no dimer; d, detectable dimer; s, significant dimer; w, as wild-type; -, not tested.

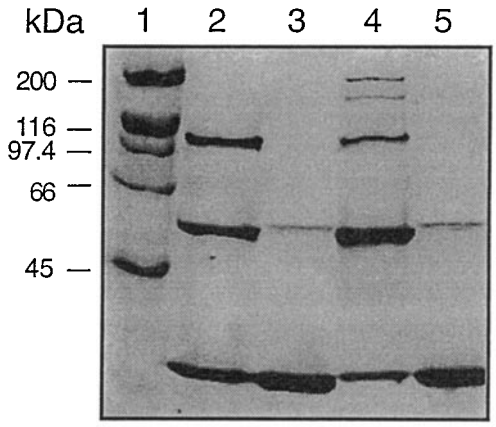

Figure 3. Gly83 but not Gly79 is important for dimer formation in mutants 3A and 4A. Lane 1: molecular mass markers. Lane 2: mutant 3A(G79L). Lane 3: mutant 3A(G83L). Lane 4: mutant 4A(G79L). Lane 5: mutant 4A(G83L).

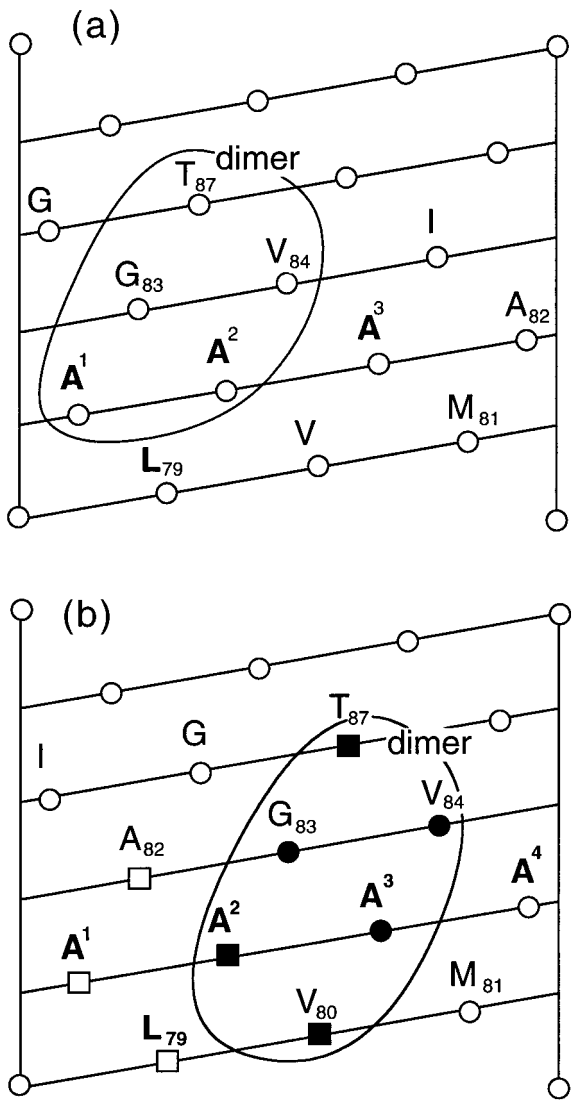

Figure 4. Helical net plots of mutant 3A(G79L) (a), and 4A(G79L) (b). Mutated residues are in bold. Positions where mutations disrupt dimer formation are filled. Positions involved in tetramer formation are indicated by squares. The putative helix-helix dimer interface is outlined. Inserted residues are indicated by superscript numbers.

for wild-type GpA, Gly83, Val84, and Thr87 belong to the dimer interface in the 4A mutant, and that dimerization increases somewhat if Gly79 is replaced by Leu. The 4A insertion thus does not restore dimerization by shifting the Gly79Val80 residues back into register but rather creates a new interface where the major difference compared to wild-type GpA is that Gly79Val80 are replaced by Ala2Ala3; similarly for the 3A insertion mutant they are replaced by Ala1Ala2 (Figure 4). In wild-type GpA, the Gly79 → Ala and Val80 → Ala mutations are only slightly disruptive, although the double mutant has not been tested. Remarkably, however, the Ala3 residue can be replaced by Trp in 4A(G79L) with no detrimental effect on dimerization, whereas the corresponding mutation Val80 → Trp is completely disruptive in wild-type GpA (Lemmon *et al.*, 1992b). As expected, replacement of Ala2 by Trp reduces the amount of dimer, though the formation of a large amount of tetramer in this mutant complicates the interpretation.

In order to test whether properties such as helical propensity or hydrophobicity might affect dimerization, insertions of five glycine residues (mutant 5G) and five leucine residues (mutant 5L) were also made between residues Met81 and Ala82. No dimer was seen for the 5G construct. Surprisingly, in contrast to the 5G and 5A mutants, 5L dimerized quite efficiently (44% dimer). Again, the additional mutation Gly83 → Leu disrupted the 5L dimer, whereas Gly79 → Leu did not (Table 1).

Since mutant 5L dimerized but 5A did not, we sought to determine which were the critical residues. When individual leucine residues were replaced by alanine, a significant increase in the amount of dimer was seen in mutant 5L(A3), whereas less dimer was found in the 5L(A4) mutant (Table 1). Conversely, the introduction of a single leucine into the 5A construct (mutant 5A(L4)) was sufficient to induce a similar level of dimerization as in the 5L mutant. The observation that mutant 5L(A3) forms more dimer than mutant 5L rules out the trivial explanation that the difference in dimerization efficiency between mutants 5L and 5A, results only from the higher helical propensity in SDS of Leu compared to Ala (Li & Deber, 1994). We conclude that dimer formation in mutants with five inserted residues involve the motif (A/L)-L-x-x-G83 and probably also Val80-Met81, Val84, and Thr87 (Figure 5). The critical

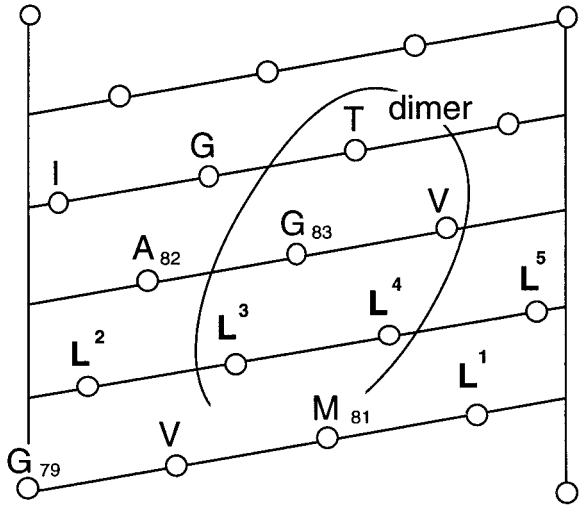

Figure 5. Helical net plot of mutant 5L. Dimer formation is abolished by the Gly83 → Leu mutation, is increased by the Leu3 → Ala mutation, and is decreased by the Leu4 → Ala mutation. The putative helix-helix interface is outlined.

Gly79Val80 motif can thus be replaced both by Ala-Leu and Leu-Leu.

Since from the data on single-site mutations in wild-type GpA the Leu-Leu mutation is predicted to be highly disruptive, we attempted to build three-dimensional models of the packing interface in the 5A, 5A(L4), 5L, 5L(A3), and 5L(A4) mutants. These models were made using the ICM program (Abagyan *et al.*, 1994), and were constrained to have an interface involving the same residue positions as in wild-type GpA (see Materials and Methods). A reasonably good correlation was found between the surface area buried in the interface in the different models and the ability of the corresponding mutants to form dimers and tetramers in SDS (Table 2) suggesting that close packing in the helix-helix interface may be the major driving force for dimerization.

Table 2. Solvent accessible surface area buried in the dimerization interface for 3D-models of GpA mutants

Constructs	Å^2	Dimer + tetramer (%)
Wild-type[a]	917	83
Wild-type[b]	894	83
5A	807	2
5A(L4)	825	53
5L	877	48
5L(A3)	914	62
5L(A4)	879	45

[a] Calculated for the wild-type model given in the PDB file 1msr.

[b] Calculated for the wild-type dimer structure modeled using the same procedure and the same constraints as were used for the modeling of the mutant structures.

Tetrameric complexes

As noted above, in certain cases rather efficient formation of tetramers occurred. In particular, we observed a dramatic increase in the amount of tetramer in mutants 4A(G79L,V80W), 4A(G79L,A1W), 4A(G79L,A2W), 4A(G79L,A82W), and 4A(G79L,T87L). Thus, Trp (and Leu) promotes tetramerization in certain positions. Although there is an apparent periodicity in the distribution of these positions, we do not feel confident to predict a structure for the tetramers from the data at hand.

It is of course difficult to rule out that tetramer formation reflects non-specific aggregation phenomena, although the dramatic difference in the amount of tetramer between closely related mutants suggests a certain degree of specificity. This is perhaps best illustrated by mutants 3A(G79L,V80W), 4A(G79L,V80W), and 4A(G79L,T87L). The first forms dimers (44%) but no tetramers, whereas the latter two form essentially no dimer but 40 to 50% tetramer, suggesting a co-operative formation of the tetramer. This is further illustrated in Figure 6, where the monomer-tetramer distribution for the 4A(G79L,V80W) mutant is shown as a function of the total protein concentration in the sample prior to loading. While the monomer-tetramer distribution shifts dramatically over this concentration range, little or no dimer is formed at any concentration.

We also sought to induce tetramer formation by duplicating all or parts of the dimer interface residues on the exposed side of the GpA transmembrane helix. While all these mutants dimerized as efficiently as wild-type GpA, only one of them (lane 5) formed a significant amount (17%) of tetramer (Figure 7(a)). In this mutant, the GVxxGVxxT part of the interface motif is duplicated, while the N-terminal Leu-Ile part is not (cf. Figure 1). Instead, we found that Ile77 and Phe78 were critical in the corresponding positions in the duplicated motif, as neither residue could be replaced by another hydrophobic residue without disrupting the tetramer (lanes 7, 8). This is in contrast to wild-type GpA, where the identity of the corresponding residues occupying positions 75 and 76 is not very critical (Lemmon *et al.*, 1992b, 1994; Mingarro *et al.*, 1996). Possibly, the lower efficiency of tetramerization compared to dimerization makes the former more sensitive to minor changes in the interface.

Considering that nearly the whole dimer interface motif needs to be duplicated and the critical importance of the Ile-Phe pair, the tetramer interface must be very similar to the dimer interface. In order to verify this, we replaced the new glycine residues (positions 81 and 85) with leucine, assuming that if the packing in the tetramer interface is similar to that in the dimer interface both mutants should disrupt the tetramer but leave the dimer intact. As shown in Figure 7(a), lanes 9 and 10, no tetramer was found in either mutant.

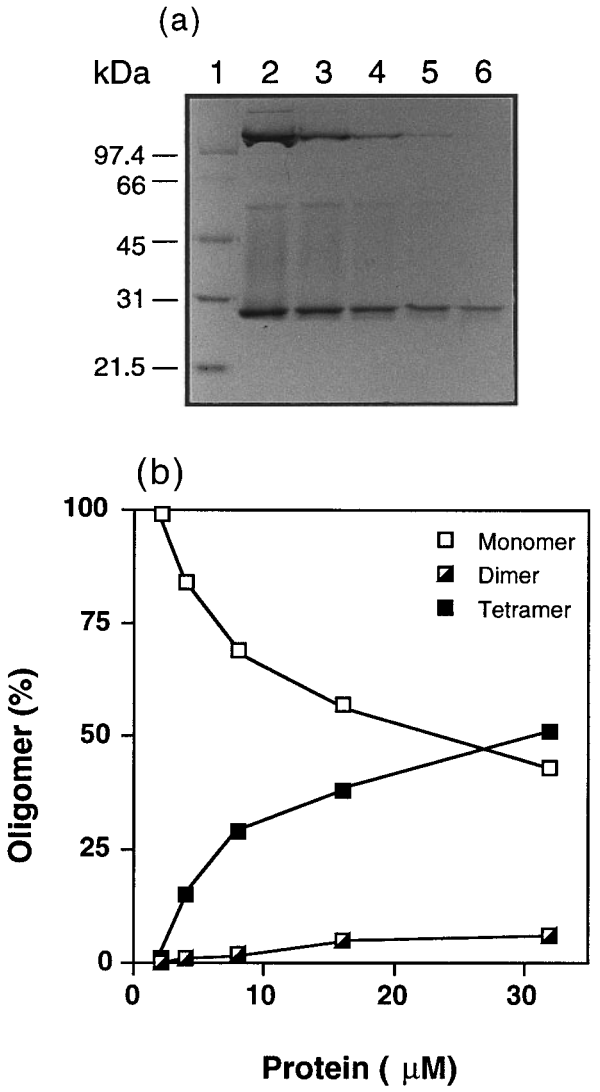

Figure 6. The monomer-tetramer distribution for mutant 4A(G79L,V80W) varies with the total protein concentration prior to loading. (a) SDS-PAGE analysis. Lane 1: molecular mass markers. Lane 2: 32 μM protein. Lane 3: 16 μM. Lane 4: 8 μM. Lane 5: 4 μM. Lane 6: 2 μM. (b) Quantitation of the data in (a).

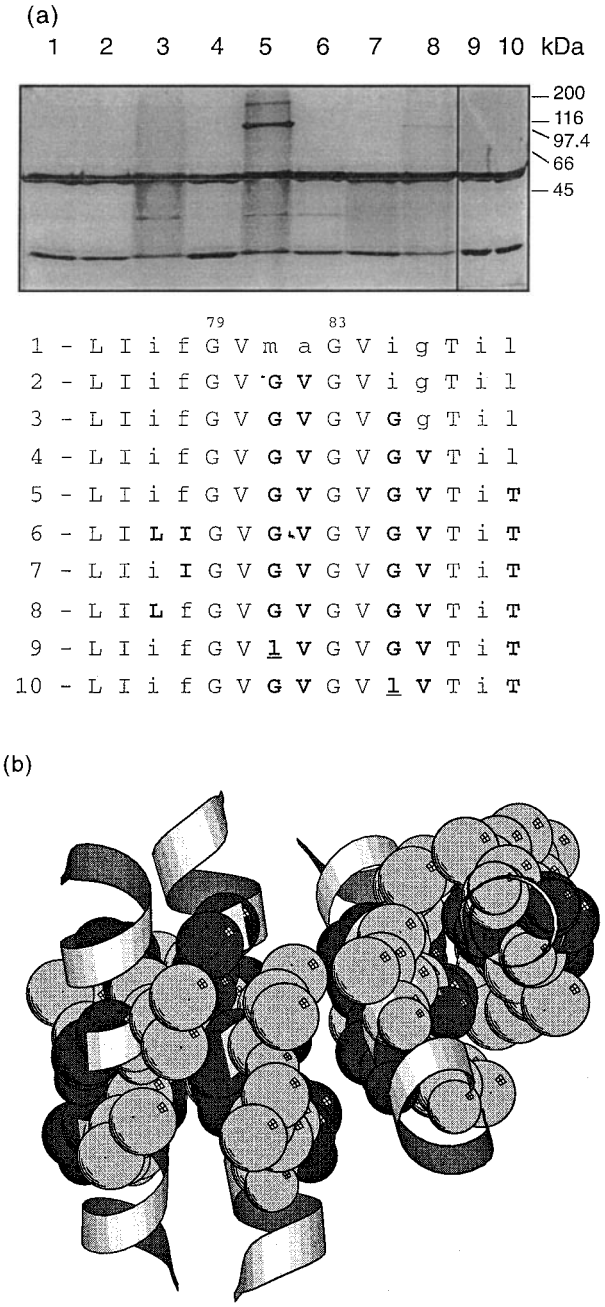

Figure 7. Tetramerization can be induced by duplication of the GpA transmembrane helix interface motif. (a) SDS-PAGE analysis of partial and complete duplication mutants. Sequence 1 is the wild-type. The original interface residues are shown in upper case, and duplicated interface residues are shown in boldface upper case. (b) Model for the tetramer (sequence 5). The interface glycine residues are shown in space filling mode in dark grey and the interface valine residues in light grey, cf. Figure 1(b).

A rough model of the tetramer based on the previously published model for the dimer (Adams *et al.*, 1996) is shown in Figure 7(b). The interacting helices in the tetramers all have roughly the same angle with respect to each other (~35°), and the rather large angle (~105°) between the two outermost helices suggests that the same kind of structure will be difficult to form in a lipid bilayer where the helices need to be more parallel.

Discussion

We have explored the sequence requirements for helix-helix packing in a non-aqueous environment by taking advantage of the known SDS-resistance of GpA dimers. Our results show that sequences with major deviations from the wild-type GpA sequence can still support efficient dimerization in detergent (Table 1), and presumably also in a natu-

ral lipid environment. It appears that the right-handed helix-helix crossing found for wild-type GpA is retained in these new dimers, and that Gly83 (and probably also Val84 and Thr87) is critical in all cases.

The Gly79-Val80 motif, on the other hand, can be replaced by Ala-Ala, Ala-Leu, Leu-Leu, Trp-Ala, and Ala-Trp, although dimerization efficiency is affected by other residues as well in these cases. Thus, although insertion of three or more alanine residues into the wild-type sequence yields interfaces with Ala-Ala replacing Gly79Val80 (Table 1), only the 3A and 4A insertions form dimers. Assuming a right-handed structure as in wild-type GpA, this means that the identity of the residues two positions upstream of the Ala-Ala pair is important, and that different residues are required in these positions depending on the choice of residues in the central pair. Thus, mutants 3A (FGvmAAaaGVigT; assumed interface residues in upper case), 4A (GVmaAAaaGVigT), and 5A(L4) (VMaaALaaGVigT) give dimers, whereas mutant 5A (VMaaAAaaGVigT) does not. Considering that mutants Leu75 → Val and Ile76 → Met are both highly disruptive in wild-type GpA (Lemmon *et al*., 1992b), it appears that the replacement of Gly79-Val80 by Ala-Leu actually increases the stability of the dimer (mutant 5A(L4)). When Gly79Val80 is replaced by Ala-Ala, on the other hand, only less disruptive deviations from the wild-type sequence in positions 75 and 76 seem to be allowed (mutants 3A and 4A *versus*. 5A). The efficient dimerization of mutant 5L (VMllLLlaGVigT) is even more surprising, as it harbors mutations in three of the critical positions (75, 76, and 79) that are all individually disruptive in wild-type GpA (note that Gly83 is still critical in this mutant). Apparently, though bulky, the leucine residues can pack quite snugly against the opposing helix, creating a rather large buried surface.

An unexpected finding in this study was that certain mutants form tetramers quite efficiently, and that two constructs form only monomer and tetramer but very little dimer (Figure 6). If the latter observation can be generalized to transmembrane helices in a lipid bilayer, it suggests that integral membrane proteins may display considerable co-operativity in their folding; a case in point is the pentameric helix bundle formed by phospholamban (Adams *et al*., 1995; Arkin *et al*., 1995). Tetramer formation could also be induced by duplication of the critical dimer interface residues on the opposite side of the GpA transmembrane helix (Figure 7). The sensitivity of tetramer formation to individual residue replacements argues against a non-specific aggregation phenomenon and suggests that precise helix-helix packing interactions are involved. This is especially clear in the case of the duplicated motif, where as little as an Ile → Leu replacement prevents tetramerization.

In summary, efficient di- and tetramerization of the GpA transmembrane helix can be induced by a wider range of sequence motifs than expected from the previous studies. The C-terminal part of the original motif, Gly83Val84/Thr87, appears to be the most critical, as all changes that we have made in these residues disrupt the dimer. The N-terminal and central residue pairs, Leu75Ile76/Gly79Val80, are much less sensitive and seem to be interdependent to some degree. This is consistent with the NMR structure of the GpA dimer (MacKenzie *et al*., 1997) which indicates that mutations in Gly83 lead to more severe steric clashes than mutations in Gly79 and in the Leu75Ile76 motif.

Materials and Methods

Plasmid constructs

Construction of the plasmids encoding the chimeric protein (SN/GpA) is described by Lemmon *et al*. (1992a). The *Hind*III-*Bam*HI fragment from pSN/GpA was cloned into the *Hind*III-*Bam*HI sites of M13mp18. For purification purposes, a His_6 tag was added by site directed mutagenesis at the extreme C terminus of the coding region. All site directed mutagenesis was performed by the Kunkel method (Kunkel, 1985) as modified by Geisselsoder *et al*. (1987). After mutagenesis, the mutated *Hind*III-*Bam*HI fragment was cloned between the *Hind*III and *Bam*HI sites in the high level expression vector pT7SN/GpA (Lemmon *et al*., 1992a).

Expression, extraction, and purification of SN/GpA

For SN/GpA production, pT7SN/GpA was transformed into *E. coli* BL21(DE3) strain containing the plasmid pLYS-S (Novagen). Colonies were picked and grown to logarithmic phase in LB at 37°C. Cultures were diluted 1:100 into terrific-broth (TB), and were grown to an A_{600} of 2.5. Isopropyl β-D-thiogalactopyranoside (IPTG) was then added to 0.8 mM, and growth was continued for a further three hours. After harvesting by centrifugation, cells were resuspended 1:20 in 50 mM Tris-HCl (pH 8), 5 mM EDTA, 1 mM phenylmethylsulfonyl fluoride (PMSF), 0.025 % (w/v) NaN_3. Cells were lyzed by three rounds of freeze-thaw in this suspension, lysis being aided by the constitutive expression of T7 lysozyme directed by the pLYS-S plasmid. $CaCl_2$ was added to 10 mM to activate the nuclease moiety of SN/GpA. The resulting cellular DNA hydrolysis was complete after incubation for 15 minutes on ice. The lysate was clarified by centrifugation, and protein was extracted from the resulting pellet by sonication for one minutes at 4°C (at 1:10 dilution) in a solution containing 20 mM Tris-HCl, 150 mM NaCl (pH 7.5; TBS), 1% (w/v) SDS, 1 mM PMSF. Non-solubilized products were removed by centrifugation and proteins were purified using Ni-NTA agarose resin (Qiagen). Samples were washed with 10 mM imidazole, 0.5% SDS in TBS and eluted with 100 mM imidazole in the same solution. The presence of the His_6 tail was found not to affect the dimerization efficiency and the chimeric product had the expected mobility on SDS-PAGE (Figure 2). Protein concentration was determined by the bicinchoninic acid protein assay (Pierce) using bovine serum albumin as a standard.

SDS-PAGE analysis

2.5 μl of a 0.66 mg/ml (25 μM) solution of purified protein was loaded onto 10 or 12% SDS polyacrylamide

gels. The loading buffer contained 2% SDS, and samples were boiled for five minutes prior to electrophoresis. Gels were stained with Coomassie blue, and the percentages of monomer and dimer were estimated by laser densitometry.

Molecular modeling

All modeling was done with the ICM program (Abagyan *et al*., 1994). The default energy function was used, with side-chain entropy terms and hydrophobicity terms turned off. The backbone of each individual helix was kept fixed in the same conformation as in the model for the GpA wild-type dimer (Adams *et al*., 1996); PDB file 1msr. All side-chain dihedral angles were allowed to vary freely, while bond length and bond angles were kept fixed. Energy minimization was performed with the standard ICM Monte Carlo program for 5000 steps.

The modeling of the different dimers shown in Table 2 was started from the PDB model of wild-type GpA and included residues corresponding to residues 74 to 91 in wild-type GpA aligned from Thr87. A distance-dependent energy function was used to keep residues that are close to each other in the original model close to each other in the final model. Specifically, all inter-helical C^{α}-pairs that are <9 Å apart in the original model were restrained using the global restraint option with the upper bound set to the original C^{α}–C^{α} distance plus 1 Å and the lower bound set to upper bound minus 5 Å. To calculate the buried surface area, the energy minimized model was compared with a model where the two helices were separated by >20 Å. The solvent accessible surface areas for both these models were calculated in ICM with a probe size of 1.4 Å (Connolly, 1983). The area buried in the dimerization interface was calculated from the difference in solvent accessible surface areas between the two models. The buried surface area for the wild-type dimer was calculated in two ways: using the PDB model, and using a model for the dimer constructed using the global restraints described above.

The modeling of the tetramer with the duplicated interface motif was started from two dimers harboring the appropriate mutations (see Figure 7(a)). All helices were kept rigid but free to move relative to each other. Distance constraints were used to make sure that the residues known to be important for dimer and tetramer formation were in close contact. The first and last residue of each helix was forced to be within 9.0 Å from the first and last residue of the neighboring helix, respectively. The C^{α} atoms of the dimer interface residues in positions 76, 79, 80, 83, and 84 were forced to be within 4.0 Å of the same residue in the second helix. In the dimer-dimer interface, the C^{α} atoms of residues 77, 81, and 85 in the second helix of the first dimer and the first helix of the second dimer were forced to be within 4.0 Å of the corresponding C^{α} atoms in the other helix.

Acknowledgments

This work was supported by an EMBO long-term postdoctoral fellowship to IM, by a grant from the Swedish Technical Sciences Research Council to AE, and by grants from the Swedish Technical Sciences Research Council, the Swedish Natural Sciences Research Council, the Swedish Cancer Foundation, and the Göran Gustafsson Foundation to GvH.

References

Abagyan, R. A., Totrov, M. M. & Kuznetsov, D. N. (1994). ICM: a new method for protein modeling and design: applications to docking and structure prediction from the distorted native conformation. *J. Comput. Chem.* **15**, 488–506.

Adams, P. D., Arkin, I. T., Engelman, D. M. & Brünger, A. T. (1995). Computational searching and mutagenesis suggest a structure for the pentameric transmembrane domain of phospholamban. *Nature Struct. Biol.* **2**, 154–162.

Adams, P., Engelman, D. & Brünger, A. (1996). Improved prediction for the structure of a dimeric transmembrane domain of glycophorin A obtained through global searching. *Proteins: Struct. Funct. Genet.* **26**, 257–261.

Arkin, I. T., Rothman, M., Ludlam, C. F. C., Aimoto, S., Engelman, D. M., Rothschild, K. J. & Smith, S. O. (1995). Structural model of the phospholamban ion-channel complex in phospholipid membranes. *J. Mol. Biol.* **248**, 824–834.

Connolly, M. J. (1983). Analytical molecular surface calculation. *J. Appl. Crystallog.* **16**, 548–558.

Geisselsoder, J., Witney, F. & Yuckenberg, P. (1987). Efficient site-directed *in vitro* mutagenesis. *BioTechniques,* **5**, 786–791.

Kraulis, P. J. (1991). MOLSCRIPT: a program to produce both detailed and schematic plots of protein structures. *J. Appl. Crystallog.* **24**, 946–950.

Kunkel, T. A. (1985). Rapid and efficient site-specific mutagenesis without phenotypic selection. *Proc. Natl Acad. Sci. USA,* **82**, 488–492.

Langosch, D., Brosig, B., Kolmar, H. & Fritz, H. J. (1996). Dimerization of the glycophorin A transmembrane segment in membranes probed with the ToxR transcription activator. *J. Mol. Biol.* **263**, 525–530.

Lemmon, M. A. & Engelman, D. M. (1994). Specificity and promiscuity in membrane helix interactions. *Quart. Rev. Biophys.* **27**, 157–218.

Lemmon, M., Flanagan, J., Hunt, J., Adair, B., Bormann, B.-J., Dempsey, C. & Engelman, D. (1992a). Glycophorin A dimerization is driven by specific interactions between transmembrane α-helices. *J. Biol. Chem.* **267**, 7683–7689.

Lemmon, M. A., Flanagan, J. M., Treutlein, H. R., Zhang, J. & Engelman, D. M. (1992b). Sequence specificity in the dimerization of transmembrane α-helices. *Biochemistry,* **31**, 12719–12725.

Lemmon, M. A., Treutlein, H. R., Adams, P. D., Brünger, A. T. & Engelman, D. M. (1994). A dimerization motif for transmembrane α-helices. *Nature Struct. Biol.* **1**, 157–163.

Li, S.-C. & Deber, C. M. (1994). A measure of helical propensity for amino acids in membrane environments. *Nature Struct. Biol.* **1**, 368–373.

MacKenzie, K. R., Prestegard, J. H. & Engelman, D. M. (1997). A transmembrane helix dimer: structure and implications. *Science,* **276**, 131–133.

Mingarro, I., Whitley, P., Lemmon, M. A. & von Heijne, G. (1996). Ala-insertion scanning mutagenesis of the glycophorin A transmembrane helix: a rapid way to map helix-helix interactions in integral membrane proteins. *Protein Sci.* **5**, 1339–1341.

Sharp, L. L., Zhou, J. & Blair, D. F. (1995a). Features of MotA proton channel structure revealed by tryptophan-scanning mutagenesis. *Proc. Natl Acad. Sci. USA,* **92**, 7946–7950.

Sharp, L. L., Zhou, J. & Blair, D. F. (1995b). Tryptophan-scanning mutagenesis of MotB, an integral membrane protein essential for flagellar rotation in *Escherichia coli*. *Biochemistry*, **34**, 9166–9171.

Treutlein, H. R., Lemmon, M. A., Engelman, D. M. & Brünger, A. T. (1992). The glycophorin A transmembrane domain dimer: sequence-specific propensity for a right-handed supercoil of helices. *Biochemistry*, **31**, 12726–12732.

Edited by F. E. Cohen

(Received 4 April, 1997; received in revised form 7 July, 1997; accepted 7 July, 1997)